

DEVELOPMENTS IN THE USE OF THE BONDED PARTICLE MODEL TO STUDY FUNDAMENTALS OF ORE FRACTURE IN MINERAL PROCESSING

LAWRENCE S. BBOSA¹, TEMITOPE OLADELE² AND DION K. WEATHERLEY³

¹Mintek
200 Malibongwe Dr, Praegville, Randburg, 2194, Gauteng South Africa
lawrenceb@mintek.co.za

²PACE
460 Portage Ave, Winnipeg, MB R3C 0E8, Canada
Postal Address

³Sustainable Minerals Institute
The University of Queensland, Brisbane QLD 4072 Australia
d.weatherley@uq.edu.au

Key words: Granular materials, DEM, Bonded particle model, dynamic loading

Abstract. In mineral processing, ore fracture is an essential first step for which the objective is to increase the exposed surface area of the valuable mineral, thereby increasing the likelihood of liberation in subsequent separation stages. This process is well known to be energy-intensive, and increasing scrutiny around sustainable practices has heightened the need to examine the efficiency of current industry approaches. Factors such as mineralogical structure and inherent weakening in the form of micro cracks are known to affect ore breakage mechanisms. However, isolating and investigating individual factors under experimental conditions is challenging and typically impractical. Numerical techniques such as the Bonded Particle Model-Discrete Element Method (BPM-DEM) have been developed as a means of investigating in isolation, the effects of different factors on ore breakage behaviour under closely controlled breakage conditions. In this work, the robustness of the BPM-DEM in predicting fracture characteristics during SILC impact breakage is evaluated. Thereafter, the BPM-DEM is used to analyse the internal mechanical response of a simulated rock specimen under impact loading commensurate with that of the SILC. The method is shown to be an insightful opportunity to study intrinsic and extrinsic rock properties during dynamic loading and breakage.

1 INTRODUCTION

Particle breakage is essential in many solid processing industries, including food, pharmaceutical, agricultural and mineral processing. In mineral processing, breakage of run-of-mine ore takes place in a comminution circuit to achieve size reduction which consequently increases the likelihood of liberation of valuable minerals [1,2]. This process is typically

associated with relatively high energy costs and is often reported to be inefficient. Previous studies have estimated that comminution typically accounts for approximately 50-60% of the total power to a plant [3], and for commonly utilized methods that less than 5% is directly utilized in the mechanics of particle breakage [4]. The sustainability of the industry necessitates improving current comminution practices, which can be facilitated through advances made from studying its fundamental mechanisms.

Impact fracture studies of single rock samples are commonly used as the initial basis to study comminution. These are normally conducted using standard laboratory breakage devices. The Short Impact Load Cell (SILC) was designed to be a portable device which could be used to determine impact breakage properties of materials at dynamic loading conditions typical to comminution devices [5].

Numerical techniques such as the discrete element method (DEM) have emerged as a means of complementing laboratory studies, acting as a “virtual laboratory” which offers the versatility to isolate and investigate highly specific scenarios. Among its strengths is the ability to alter its parameters in a carefully calibrated environment and examine their effect in isolation on the types of macro scale responses measured by experiments. Furthermore, DEM has been demonstrated as a viable tool for studying fracture mechanics in many forms including rock blasts, seismic failures and within comminution devices [6,7,8].

Based on these considerations, this study aimed to evaluate the robustness of the BPM-DEM in predicting fracture characteristics during SILC impact breakage. Thereafter, the BPM-DEM was used to analyse the internal mechanical response of a simulated rock specimen under impact loading commensurate with that of the SILC. Thereby, the BPM-DEM was demonstrated to be a beneficial approach which provides an opportunity to study both intrinsic and extrinsic rock properties during dynamic loading and breakage.

2 SUMMARY OF METHODOLOGY

2.1 Discrete element method

The discrete element method (DEM) is a discontinuous numerical modelling approach based on Newton’s laws of mechanics, initially designed to study the flow of granular materials [9]. A physical system is represented as an assembly of discrete entities, typically spheres, referred to as DEM-spheres in this work. These DEM-spheres undergo forces due to prescribed interactions with adjacent DEM-spheres, other entities such as walls, and/or potential fields such as gravity.

The method explicitly computes the net force acting on each DEM-sphere at an instantaneous time and subsequently updates the positions and velocities of the DEM-spheres to the next discrete time step by integrating the ensuing equation of motion (Newton’s Second Law; Eq. 1). Typically, explicit time-integration schemes are employed, allowing dynamic processes such as elastic wave propagation to be simulated. In cases where only the quasi-static response of materials is of interest, artificial damping forces are added to approximate implicit time-integration; an approach similar to penalty methods employed in continuum numerical models.

The instantaneous acceleration of any given DEM-sphere i is given by the sum of all forces acting on that DEM-sphere at a prescribed time t . The basic forces are DEM-sphere-pair

interactions (F_{ij}^p), damping (F_i^d) and gravitation (F_i^g), as well as wall forces (F_i^w), although other expressions can be added depending on the scenario to be simulated.

$$m_i \frac{dv_i}{dt} = \sum_{j=1}^{N_i^c} F_{ij}^p + F_i^d + F_i^g + \sum_{w=1}^{N_w} F_i^w \quad (1)$$

Where: m_i , v_i are the mass and velocity of DEM-sphere i at time t . Furthermore, N_i^c indicates the total number of DEM-spheres in contact with DEM-sphere i and N_w is the number of walls within the simulation domain.

This equation of motion is typically integrated in time via one of a range of explicit numerical time integration schemes (Eqs 2 and 3). One of the simplest such schemes is employed herein:

$$v_i(t + \Delta t) = v_i(t) + \Delta t \frac{dv_i}{dt}(t) \quad (2)$$

$$p_i(t + \Delta t) = p_i(t) + \Delta t v_i(t + \Delta t) + \Delta t^2 \frac{dv_i}{dt}(t) \quad (3)$$

Where: p_i is the position of DEM-sphere i and Δt is the time-step increment.

As the DEM has been refined, it has proven useful to model a variety of applications in highly dynamic scenarios involving high particle strain rates [10,11,12]. Examples include; earth quake studies and fault propagation [13], rock fracture [14,15] and comminution [16,17]. Many such scenarios necessitated the implementation of breakage modelling within the DEM environment, in addition to contact mechanics appropriate for simulating granular media.

2.2 Bonded particle model

The BPM represents a parent particle as an assembly of DEM-spheres each bound to neighbours via brittle-elastic beam interactions. Upon application of external forces to the assembly of bonded particles, each beam interaction is stressed until a prescribed failure criterion is met. Beam interactions meeting the failure criterion are replaced with elastic repulsive, frictional interactions between the previously bound particles; the compressive and shear elastic stiffnesses of which match that of the replaced beam interactions. This method aims to mimic the spontaneous formation of frictional fracture surfaces during crack propagation within brittle materials. Consequently, the shapes and size-distributions of progeny particles arise naturally and can therefore be validated with reference to laboratory experiments.

The simplest BPM models employ simple linear elastic springs between adjacent DEM-spheres, with failure occurring when the spring extension exceeds a prescribed distance. These simple BPMs accurately simulate failure of brittle materials under pure tension but do not accurately predict crack propagation under compressive or shear loading. The latter is achieved by accounting for additional deformational degrees-of-freedom between adjacent DEM-spheres; specifically shear, bending and torsional deformation in addition to tensile/compressive deformation. A variety of mathematical formulations have been proposed to accommodate these additional degrees-of-freedom, although the exact details of the formulation appear to be of little importance for simulating crack propagation and failure of brittle materials. Herein, the formulation of Wang et al. [12] is employed.

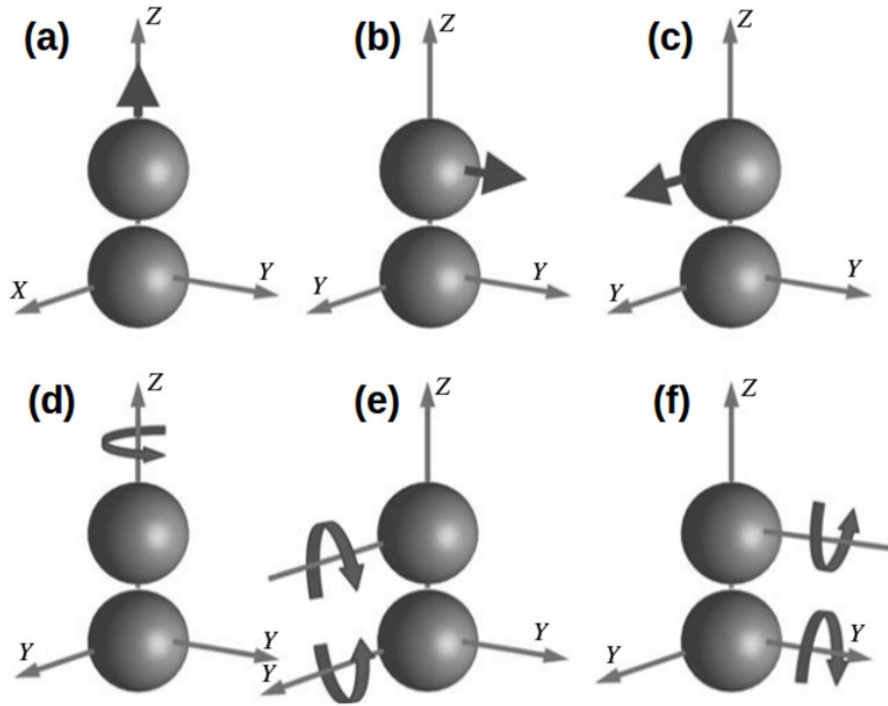


Figure 1: The six interactions between bonded DEM-spheres: pulling or pushing in radial direction (a), shearing forces in tangential direction (b and c), twisting (d) and bending around two axis (e and f). Wang et al., (2006)

Wang et al notionally connect adjacent DEM-spheres with cylindrical linear elastic beams having six deformational degrees-of-freedom, as illustrated in Fig. 1. Each degree-of-freedom is mathematically represented via a Hookean interaction. Purely tensile (compressive) forces are proportional to the relative extension (compression) of adjacent DEM-spheres. Similarly shear forces in each of the two directions perpendicular to the line joining the two DEM-sphere's centres-of-mass are calculated in proportion to the relative shear displacement. Ascribing an initial orientation to each DEM-sphere (rotational degrees-of-freedom in addition to translational) permits the calculation of relative bending and twisting between adjacent DEM-sphere; with bending and twisting moments calculated in proportion to the relevant changes in angle between adjacent DEM-spheres.

With the assumption of isotropy of shearing and bending deformation, two forces (Eqs 5 and 6) and two moments (Eqs 7 and 8) are calculated between adjacent, bonded pairs of DEM-spheres, in any given timestep. These are:

$$F_{ij}^n = K_{ij}^n \Delta U_{ij}^n \quad 4$$

$$F_{ij}^s = K_{ij}^s \Delta U_{ij}^s \quad 5$$

$$M_{ij}^b = K_{ij}^b \Delta \theta_{ij}^b \quad 6$$

$$M_{ij}^t = K_{ij}^t \Delta \theta_{ij}^t \quad 7$$

Where: ΔU_{ij}^α is the relative normal or shear ($\alpha = n$ or s) displacement of adjacent DEM-spheres i and j , and $\Delta\theta_{ij}^\beta$ is the relative angle change due to bending or torsion ($\beta = b$ or t) between the DEM-spheres.

The four spring constants ($K_{ij}^n, K_{ij}^s, K_{ij}^b, K_{ij}^t$) are computed in accordance with linear elastic beam theory given by Eqs 9-12. Assuming adjacent DEM-spheres are connected via cylindrical beams whose cross-sectional radius is equal to the arithmetic mean of the radii of the DEM-spheres [$R_{ij} = \frac{1}{2}(R_i + R_j)$] and whose equilibrium length is equal to the sum of the DEM-sphere radii:

$$K_{ij}^n = \frac{\pi}{2} Y (R_i + R_j) \quad 8$$

$$K_{ij}^s = \frac{\pi}{2} G (R_i + R_j) \quad 9$$

$$K_{ij}^b = \frac{\pi}{8} Y (R_i + R_j)^3 \quad 10$$

$$K_{ij}^t = \frac{\pi}{4} G (R_i + R_j)^3 \quad 11$$

Where: Y is the interaction Young's modulus and $G = \frac{Y}{2(1+\nu)}$ is the interaction shear modulus; typically defined in terms of a dimensionless Poisson's ratio (ν). It should be noted that these mechanical parameters are micro-physical quantities. The equivalent macroscopic mechanical properties are related to these but also depend upon the topology of the assembly of bonded interactions comprising a DEM rock sample.

Failure of bonded interactions is governed by a Mohr-Coulomb failure criterion shown in Eq 13.

$$\tau_{ij} \geq \begin{cases} C - \sigma_{ij}^n \tan \Phi & \text{if } \sigma_{ij}^n < C \tan \Phi \\ 0 & \text{otherwise} \end{cases} \quad 12$$

Where: C is the cohesive strength of the interaction and Φ is the internal angle of friction. The normal stress (σ_{ij}^n) and shear stress (τ_{ij}) of the interaction are computed in accordance with linear elastic beam theory expressed Eqs 14 and 15 respectively:

$$\sigma_{ij}^n = \frac{F_{ij}^n}{A_{ij}} + \frac{|M_{ij}^b|}{I_{ij}} R_{ij} \quad 13$$

$$\tau_{ij} = \frac{|F_{ij}^s|}{A_{ij}} + \frac{|M_{ij}^t|}{J_{ij}} R_{ij} \quad 14$$

Where: $A_{ij} = \pi R_{ij}^2$ is the cross-sectional area, $I_{ij} = \pi R_{ij}^4/4$ is the bending moment of inertia and $J_{ij} = \pi R_{ij}^4/2$ is the polar moment of inertia of the interaction connecting DEM-spheres i and j .

3 NUMERICAL APPROACH

Numerical simulations were conducted using ESyS-Particle, an open-source discrete element method (DEM) software package which uses Python-based libraries to generate geometries and simulations and a C++ engine for mathematical computations

(<https://launchpad.net/esys-particle>). Sample geometries were created using Gengeo, a library of tools available within the ESYs-particle package. which uses a volume-filling algorithm to pack DEM-spheres into a prescribed volume. The numerical methodology employed herein consists of the following two steps: model calibration and numerical SILC experiments. These are described in the sections that follow.

4 INITIAL STATISTICAL ANALYSIS OF FRACTURE CHARACTERISTICS

4.1 Model resolution sensitivity analysis

Model resolution has been demonstrated to have a significant effect on the accuracy of BPM simulations of rock damage [18]. The effect of model resolution in this current study was examined by varying the scale of DEM-spheres and measuring the variation in fracture force obtained while keeping all other simulation parameters constant. Model resolution herein is governed by a dimensionless ratio (R_{max}/L) i.e., the ratio of the maximum radius of DEM-sphere in the simulation (R_{max}) to the length of the specimen (L), where L is constant.

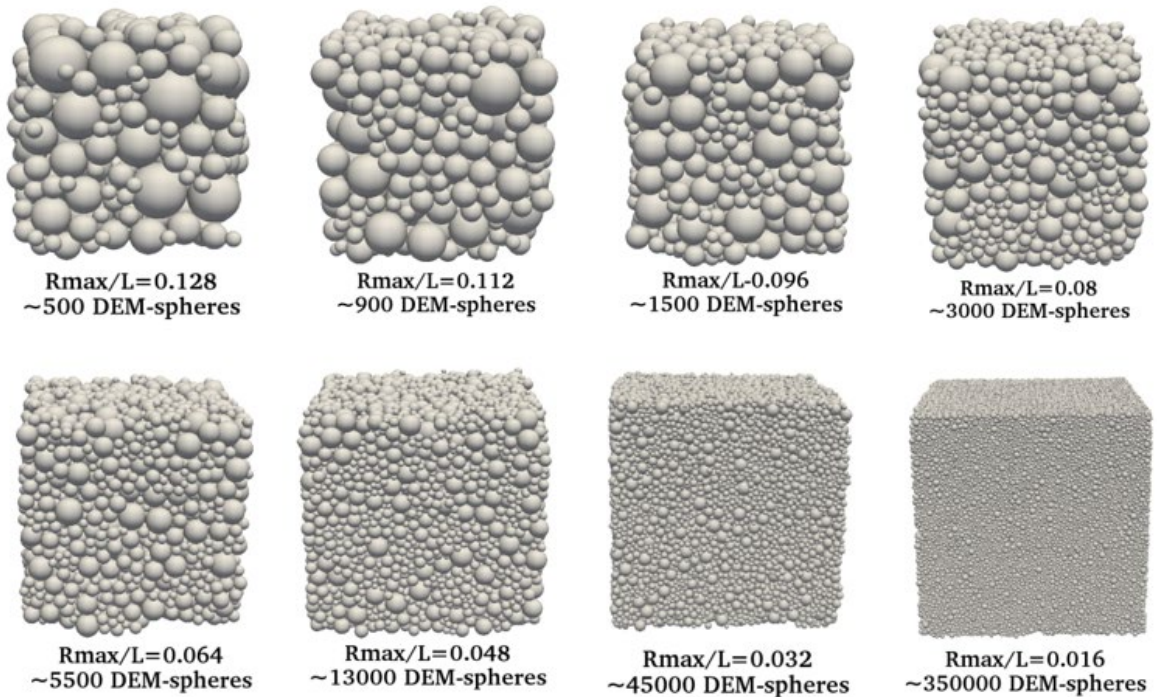



Figure 2: A representative specimen at different model resolutions

It is important to emphasize that the resolution level was indicated by the number of DEM-spheres, whereby fewer spheres translated to lower levels while a greater number meant a higher level. Model resolution was varied from 0.128 (low level) to 0.016 (high level) to test scenarios from relatively low to high amounts of DEM-spheres, as demonstrated in Fig.3. For each resolution, an equal ratio between the minimum DEM-sphere radius (R_{min}) and R_{max} was maintained. This ensures that the macroscopic mechanical properties of the rock specimens remain the same. Each simulation was repeated 30 times to provide representative statistics for each scenario.

Table 1 lists the parameters used for both R_{min} and R_{max} at different model resolutions as well as the approximate average number of DEM-spheres obtained when the numerical volume filling algorithm completed constructing the specimens. In addition, the mean fracture force and indication of the variation is given. The average fracture force remained statistically consistent for all model resolutions except the lowest two levels. The variation in fracture force tended to increase at successively lower model resolution levels, with the lowest two exhibiting notably wider discrepancies.

Table 1: Example of the construction of one table

Rmin (mm)	Rmax (mm)	Rmax/L	Approx. No. DEM- spheres	Average Fracture force (kN)	Std Dev	Resolution Level
0.32	1.28	0.128	550	5.15	1.56	Lowest
0.28	1.12	0.112	900	4.65	1.49	
0.24	0.96	0.096	1500	4.04	1.06	
0.20	0.80	0.080	3000	3.84	0.77	
0.16	0.64	0.064	5500	3.93	0.95	
0.12	0.48	0.048	1300	3.65	0.59	
0.08	0.32	0.032	45000	3.39	0.47	
0.04	0.16	0.016	350000	3.04	0.18	

This implied that the measured fracture force converged to greater accuracy with higher model resolution, highlighting the importance of selecting a sufficient size and number of DEM-spheres when used to represent a rock specimen.

4.2 Specimen-size dependency

The sensitivity of the BPM to specimen size when calculating fracture characteristics was also investigated by varying lengths from 2-10mm. Simulations across different rock specimen lengths were conducted at a resolution (R_{max}/L) of 0.032, which was noted to give reasonably accurate representation in the previous section. An added advantage of this model resolution was increased computational efficiency, with simulations at this level requiring 15 hours per specimen in comparison with approximately double the time per specimen at the highest resolution.

Figure 3 shows a summary plot of the variation in fracture force with size. This depicted a non-linear size dependency with fracture force, in accordance with theory, and progressively increasing variation in fracture force as rock specimen length increased.

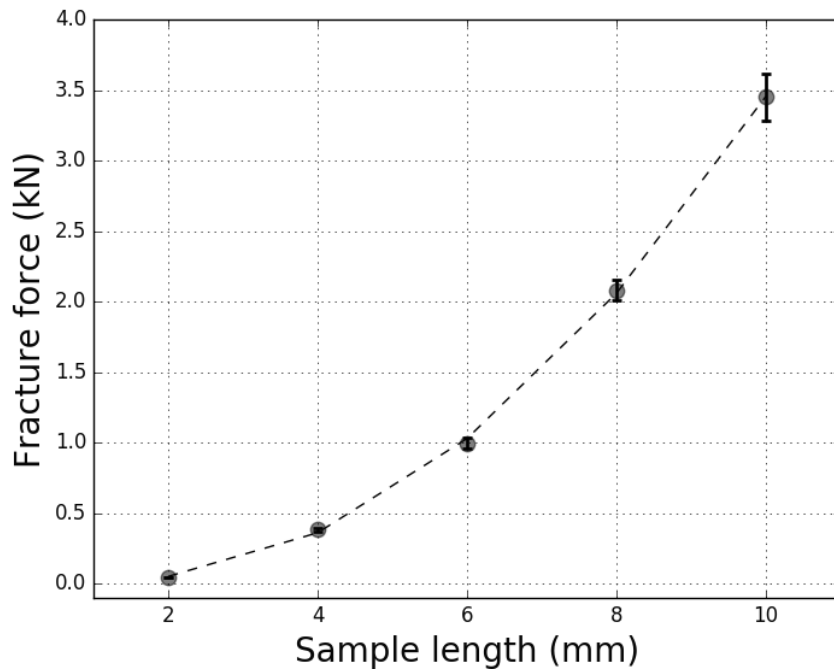


Figure 3: Variation of fracture force with specimen length

5 MEASUREMENT OF MECHANICAL PROPERTIES

Following the evaluation of variability in the BPM-DEM model, a study was considered to assess the integrity of the technique in performing impact breakage SILC simulations on a 10mm cylindrical rock specimen. The macro-scale responses were extracted and analyzed with the added benefit of concurrently examining the microscale behaviour. Pertinent information included force-time histories, extent of new free surface generation (inferred from the percentage of broken bonds/beams joining DEM spheres together) and stress (stress tensor within the simulation domain).

Figure 4 (left) provides a comparison plot of the force and percentage of broken bonds across the duration of the impact, with the stress tensor and extent of fracture at the instance of fracture shown on the right. The behavior of the simulations followed closely that typically observed in SILC experiments.

The steel ball contacted the rock sample at the start of impact, resulting in a gradual increase in the measured force as stress intensified toward a maximum. As the stress built up, an increasing number of connecting bonds began to break as illustrated, representing the gradual accumulation of damage to the sample at locations which could be spatially visualized. Over the duration of fracture, the percentage of broken bonds increased drastically corresponding to the point of failure (peak fracture force) and subsequent cleaving of the sample largely into two halves.

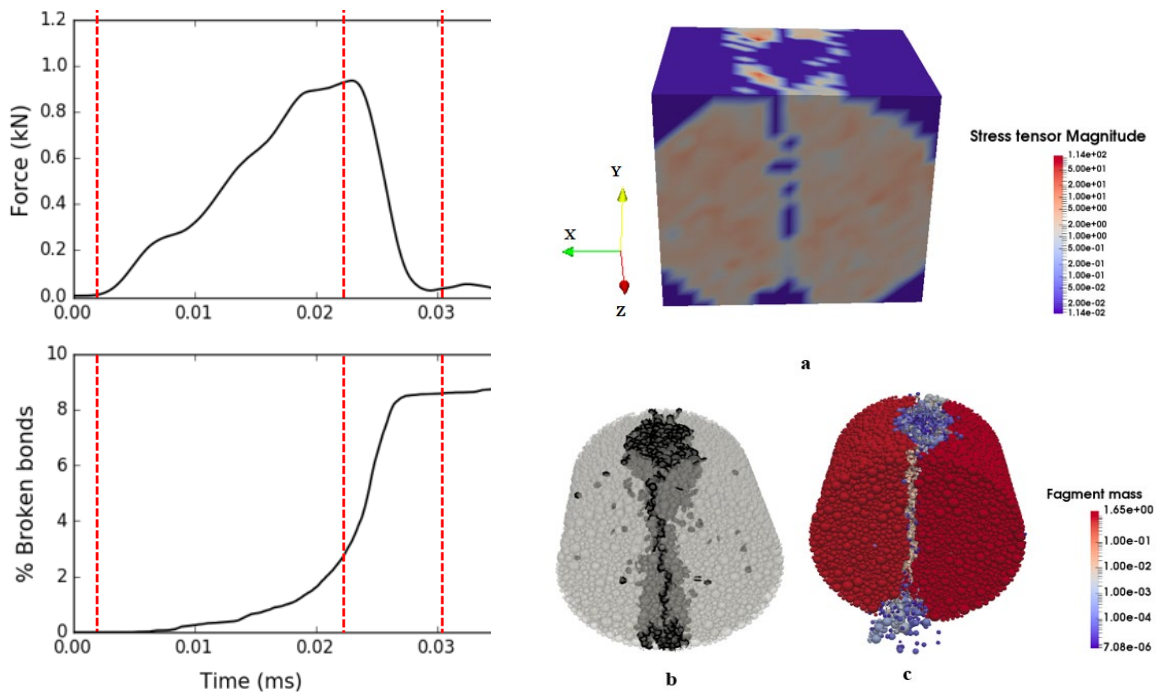


Figure 4: Plots of the force and percentage of broken bonds over the duration of impact (left), with the stress tensor magnitude and fracture shown at 0.028s (right).

The Young's modulus (Y) and uniaxial compressive strength (UCS) are important macro mechanical material properties in rock mechanics. While Y describes the elastic property of a rock specimen prior to failure, the UCS is commonly quantified as the strength. The sensitivity of these characteristics in the current setup was investigated. Figure 5 provides plots of the fracture force against the UCS and Y respectively obtained from systematically varying these over a spectrum of normally observed values. 350 simulations were conducted with ten specimens in each combination of UCS and Y .

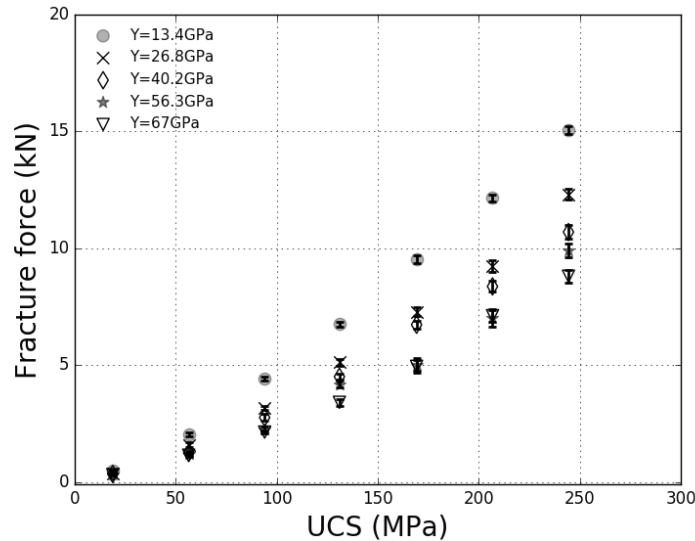


Figure 5: Fracture force versus UCS at different Young's moduli

6 DISCUSSION

This study evaluated the bonded particle model in DEM for simulating common scenarios of rock breakage under dynamic loading in a SILC device. The robustness of this model was initially tested by considering model resolution sensitivity, size dependency and ranges of variation of macroscopic mechanical properties against measured fractured characteristics.

The number of discrete entities (DEM-spheres) is a simplified representation of the microstructure of a typical rock. The current investigation highlights that a high model resolution (i.e. a higher number of entities used to construct the rock) has a significant effect on reducing the variation associated with the obtained fracture characteristics. This indicates that prior to performing simulations it is worth considering whether the selected configuration is numerically “safe” to obtain consistent and realistic results. This approach can be further refined to align it with actual measurements by integrating mineralogical data from techniques such as X-ray computed tomography [19]. In this way, approximated grain sizes could be used as a basis to define the R_{min} and R_{max} parameters as well as the composition used for simulations. The current work assumed a constant ratio of R_{min} and R_{max} for simplicity. Size dependency is another criterion to consider when testing model sensitivity. Larger sizes typically lead to greater variability in the fracture response, with experimental literature concurring that larger rock specimens increase the likelihood of containing flaws and inconsistencies in the application of loading.

7 SUMMARY AND CONCLUSION

The BPM-DEM has been demonstrated to be a robust breakage model that provides an opportunity to study both intrinsic and extrinsic rock properties during dynamic loading and breakage. Model resolution, rock specimen size and the variance of macro and micro-mechanical properties were statistically analysed to benchmark the integrity of the initial case.

Selecting a model resolution with a sufficiently high number of DEM-spheres to produce consistent results was demonstrated to be an important step toward achieving numerically stable results. The dependence of some fracture characteristics on rock specimen size highlighted how some variabilities observed during ore characterization tests may be size effects. It was also shown that the macro level properties such as Young’s modulus and UCS could be tuned to desired values, i.e. representing a wide range of ore types.

Inclusion of increasingly representative features will facilitate the use of the BPM for quantitative investigations on the relationships between ore properties, the form of load application, and its macroscopic mechanical response; knowledge that will enable future analytical ore characterisation methodologies to supplant contemporary empirical methods.

REFERENCES

- [1] Wills, B.A. and Napier-Munn, T. *Wills' Mineral Processing Technology: An Introduction to the Practical Aspects of Ore Treatment and Mineral Recovery*. Butterworth-Heinemann, (2015).
- [2] Fuerstenau, M.C. and Han, K.N. *Principles of Mineral Processing*. SME, (2003).
- [3] Ballantyne, G.R. and Powell, M.S. Benchmarking Comminution Energy Consumption for the Processing of Copper and Gold Ores. *Minerals Engineering*, 65:109-114, (2014).

- [4] Tromans, D. Mineral Comminution: Energy Efficiency Considerations. *Minerals Engineering*, 21(8):613-620, (2008).
- [5] Bourgeois, F.S. and Banini, G.A. A Portable Load Cell for In-situ Ore Impact Breakage Testing. *International Journal of Mineral Processing*, 65(1):31-54, (2002).
- [6] Weatherley, D. and Ayton, T. Numerical Investigations on the Role of Micro-cracks in Determining the Compressive and Tensile Strength of Rocks. *EGU General Assembly Conference Abstracts*, 8294, (2012).
- [7] Weerasekara, N.S., Powell, M.S., Cleary, P.W., Tavares, L.M., Evertsson, M., Morrison, R.D., Quist, J. and Carvalho, R.M. The Contribution of DEM to the Science of Comminution. *Powder Technology*, 248:3-24, (2013).
- [8] Han, Z., Weatherley, D. and Puscasu, R. Application of Discrete Element Method to Model Crack Propagation. *13th ISRM International Congress of Rock Mechanics, International Society for Rock Mechanics*, (2015).
- [9] Cundall, P.A. and Strack, O.D. A Discrete Numerical Model for Granular Assemblies. *Geotechnique*, 29(1):47-65, (1979).
- [10] Wang, Y., Yin, X., Ke, F., Xia, M. and Peng, K. Numerical Simulation of Rock Failure and Earthquake Process on Mesoscopic Scale. *Pure and Applied Geophysics*, 157(11-12):1905-1928, (2000).
- [11] Griffiths, D.V. and Mustoe, G.G. Modelling of Elastic Continua Using a Grillage of Structural Elements Based on Discrete Element Concepts. *International Journal for Numerical Methods in Engineering*, 50(7):1759-1775, (2001).
- [12] Wang, Y., Abe, S., Latham, S. and Mora, P. Implementation of Particle-scale Rotation in the 3-D Lattice Solid Model. *Pure and Applied Geophysics*, 163(9):1769-1785, (2006).
- [13] Mora, P. and Place, D. A Lattice Solid Model for the Nonlinear Dynamics of Earthquakes. *International Journal of Modern Physics C*, 4(06):1059-1074, (1993).
- [14] Hentz, S., Donzé, F.V. and Daudeville, L. Discrete Element Modelling of Concrete Submitted to Dynamic Loading at High Strain Rates. *Computers & Structures*, 82(29-30):2509-2524, (2004).
- [15] Potyondy, D.O. and Cundall, P.A. A Bonded-particle Model for Rock. *International Journal of Rock Mechanics and Mining Sciences*, 41(8):1329-1364, (2004).
- [16] Huang, H., Detournay, E. and Bellier, B. Discrete Element Modelling of Rock Cutting. *Rock Mechanics for Industry*, 1(1):123-130, (1999).
- [17] Cleary, P.W. DEM Simulation of Industrial Particle Flows: Case Studies of Dragline Excavators, Mixing in Tumblers and Centrifugal Mills. *Powder Technology*, 109(1-3):83-104, (2000).
- [18] Charikinya, E. Characterising the Effect of Microwave Treatment on Bio-Leaching of Coarse, Massive Sulphide Ore Particles. *PhD thesis, University of Stellenbosch, South Africa*, (2015).
- [19] Ghorbani, Y., Becker, M., Petersen, J., Morar, S.H., Mainza, A. and Franzidis, J. Use of X-ray Computed Tomography to Investigate Crack Distribution and Mineral Dissemination in Sphalerite Ore Particles. *Minerals Engineering*, 24(12):1249-1257, (2011).